OUTFLOW ANGLE FOR SIDE WEIRS IN A CHANNEL WITH MOBILE BED AT FLOOD DISCHARGES

Burkhard Rosier[1], Jean-Louis Boillat[2] and Anton J. Schleiss[3]

ABSTRACT

In flood protection engineering, side weirs or overflow dams are used to divert water in a controlled way into flood plains as soon as the discharge capacity of the channel is reached.
Due to the lateral loss of water the sediment transport capacity in the main-channel is reduced yielding to aggradation and the formation of a local sediment deposit in the downstream weir alignment. The reduced cross section generates backwater effects through contraction and expansion losses. Accompanied with supplementary roughness induced by bed forms the side overflow increases in an uncontrolled way, since the extent of the morphological bed changes is not known a priori.
Designing side weirs, an appropriate knowledge of the lateral outflow angle plays an important role, e. g for the determination of the side weir discharge coefficient. Based on an extensive flume study, an expression for the outflow angle is developed and compared with approaches from literature. The simple and explicit structure of the relationship incorporating channel, weir and flow parameters allows the sound application in engineering practice.

Keywords: Side weir, bed morphology, local deposition, overflow angle, flood protection.

INTRODUCTION

Side overflows are free overflow regulation and diversion devices commonly encountered in hydraulic engineering. They are set into the side of a channel, river or dam allowing to spill a part of the discharge over their crest when the surface of the flow in the main-channel or reservoir exceeds a certain level.

In river engineering usually mobile bed conditions are present and significant morphological bed changes might be induced by the side overflow device. Commonly, the lateral loss of water takes place on a rather short stretch. Consequently, the main-channel discharge and thus the bottom shear stress and the sediment transport capacity in the main-channel are suddenly reduced. As a result aggradation and the formation of a local sediment deposit near the weir or dam alignment can occur. The increase of the mean bed elevation generates backwater effects. In addition, the local sedimentary deposit induces both, horizontal and vertical energy losses through contraction and expansion phenomena. Furthermore, the mobile bed surface might be covered with alluvial bed forms increasing the overall flow resistance compared to

1 Research associate, Laboratory of Hydraulic Constructions (LCH), Swiss Federal Institute of Technology (EPFL), EPFL-ENAC-ICARE-LCH, GC A3 504, Bâtiment GC, Station 18, 1015 Lausanne, Switzerland (Tel.: +41-21-693-6338, Fax: +41-21-693-2264; email: burkhard.rosier@epfl.ch)
2 Senior research associate, LCH-EPFL (email: jean-louis.boillat@epfl.ch)
3 Professor and director, LCH-EPFL (email: anton.schleiss@epfl.ch)

plane bed conditions. As a consequence, the upstream water level and the pressure head above the side overflow device rise and the spill discharge as well. Hence, the design discharge to be diverted over the weir is increased in an unforeseen way by this flow-sediment transport interaction.

The flow over a side weir is a typical case of spatially varied flow with decreasing discharge and has been subject to numerous investigations (e. g. Subramanya & Awasthy, 1972 and Hager, 1987). Usually, the main design objective is to estimate the total overflow discharge. Therefore, the focus of research is laid on the determination of an appropriate discharge coefficient. All contributions have in common that a fixed channel bottom is assumed, since most studies refer to irrigation or drainage engineering. Especially in natural rivers a mobile bed is present and for the purpose of flood control management its morphological behaviour has to be taken into account.

Due to the lack of knowledge regarding the interaction of a side overflow with bed-load and bed morphology in a channel systematic flume experiments have been performed. Investigating the morphological phenomena like aggradation and local sediment deposition one point of interest is the behavior of the lateral outflow angle under mobile bed conditions. This topic is of considerable importance, since in the determination of the side weir discharge coefficient, and hence the side overflow intensity, the lateral outflow angle might play a significant role (Subramanya & Awasthy, 1972).

Moreover, the hydraulic stresses exerted from the overflow on the side overflow structure itself, e. g. a weir, the body of an overflow dam or the flow-side bank protection layer (concrete, blocs, vegetation or other), especially in the overflow region (crest region), depend, amongst other parameters, on the orientation of the approaching flow relative to the weir, and hence on the lateral outflow angle.

THEORETICAL CONSIDERATIONS

Assuming a constant specific energy (E) along a channel ($S_0 - S_f = 0$ with S_0 bottom slope and S_f friction slope, Fig. 1a), the discharge over a side weir per unit length (q_D) is given by (e. g. Subramanya & Awasthy, 1972):

$$q_D = \frac{2}{3} C_D \sqrt{2g} \left(y - w_D \right)^{3/2} \tag{1}$$

with C_D side weir discharge coefficient known as the De Marchi coefficient (C_M), g acceleration due to gravity, y flow depth and w_D side weir crest height. Eq. 1 represents the general equation of weirs.

Considering an elemental length dx of the side weir in the plan view (Fig. 1c) and using Eq. 1, the outflow through this elemental length is:

$$Q_D = q_D \, dx = \frac{2}{3} C_D \sqrt{2g} \, dx \, y^{3/2} \tag{2}$$

Therefore, $w_D = 0$. This flow can also be considered as a deflected jet and as such the effective width of the jet normal to the velocity vector would be (Fig 1c):

$$dx_D = dx \, \sin \phi_D \tag{3}$$

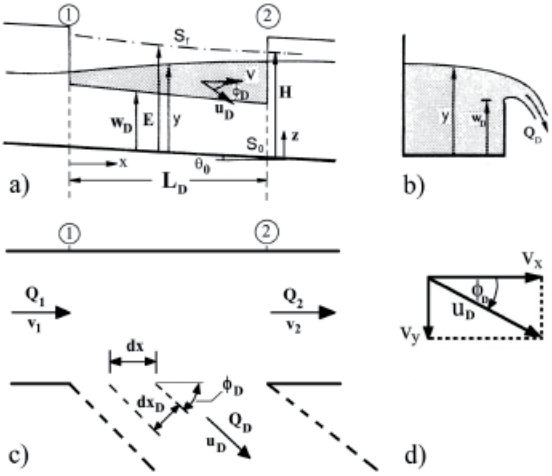

Fig. 1: Definition sketch of geometrical and hydraulic main-channel and side weir parameters: a) longitudinal section, b) cross section, c) plan view and d) definition of the lateral outflow angle ϕ_D. a) and b) are taken from Sinniger & Hager (1989), modified

Consequently, Eq. 2 can be written as:

$$Q_D = \frac{2}{3} C_D^* \sqrt{2g}\ dx\ \sin\phi_D \tag{4}$$

with C^*_D constant coefficient representing the coefficient of contraction.

Side weirs are structures in which flow conditions vary gradually. Therefore, the head losses due to wall friction and lateral outflow are small and approximately potential flow conditions with a nearly uniform velocity distribution may be assumed (Hager, 1987). Accordingly, the average channel velocity (v) and the axial component of the lateral outflow velocity ($u_D \cos \phi_D$) are equal; $v = u_D \cos \phi_D$ (Favre, 1933). Expressing $\cos \phi_D = (1 - \sin^2 \phi_D)^{1/2}$ then yields:

$$\sin\phi_D = \sqrt{1 - \left(\frac{v}{u_D}\right)^2} \tag{5}$$

As the flow situation is similar to that of a flow over a brink in a channel drop (Subramanya & Awasthy, 1972), it might be assumed that the critical depth corresponding to q_D occurs at the plane of the side weir of zero height, such that the critical velocity (v_c) is given by:

$$\frac{v_c^2}{2g} = \frac{1}{3} E = \frac{1}{3}\left(y_1 + \frac{v_1^2}{2g}\right) \tag{6}$$

Substituting $v_c = u_D$ and noting $Fr_1^2 = v_1^2 / (g\ y_1)$:

$$\sin\phi_D = \sqrt{1 - \frac{3Fr_1^2}{2 + Fr_1^2}} \tag{7}$$

Thus, from Eqs 2, 4 and 7 follows:

$$C_D = C_D^* \sqrt{1 - \frac{3Fr_1^2}{2 + Fr_1^2}} \tag{8}$$

The value of C^*_D can be chosen as 0.611 as it represents the contraction coefficient due to an efflux from a construction with $Fr_1 \rightarrow 0$ (Subramanya & Awasthy, 1972).

Finally, the side weir discharge coefficient according to Subramanya & Awasthy (1972) reads:

$$C_D = 0.611 \sqrt{1 - \frac{3Fr_1^2}{2 + Fr_1^2}} \tag{9}$$

From these theoretical considerations it can be concluded that the lateral outflow angel (ϕ_D, Eq. 7) is directly implemented in the side weir discharge coefficient according to Subramanya & Awasthy (1972) (Eq. 9), and hence plays a substantial role in the determination of the side overflow discharge according to Eq. 1.

The lateral outflow angle is also implicitly incorporated in the derivation of the side weir discharge coefficient according to Hager (1987).

EXPERIMENTS

The experiments were conducted in a rectangular 30 m long, 2.0 m wide, and 1.5 m deep glass-sided main flume (Fig. 2). The main flume was subdivided longitudinally into two separate channels. The first one, being 1.5 m wide, represents the actual testing facility with the mobile bed (d_{50} = 0.72 mm) and the side weir. The second one, 0.47 m wide, constitutes a lateral channel enabling to evacuate the diverted discharge.

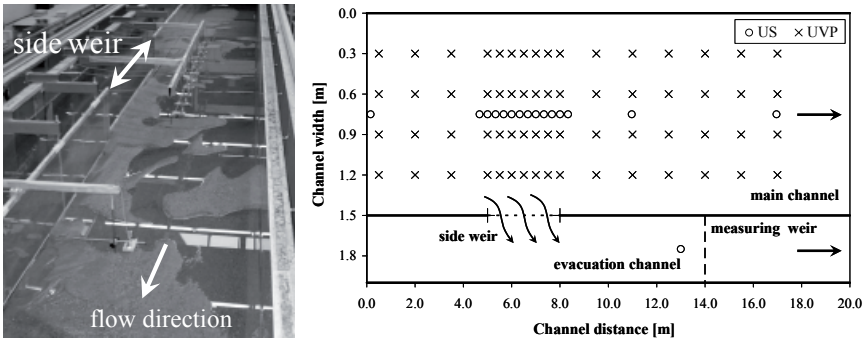

Fig. 2: Left: Laboratory setup with main-channel, mobile bed, side weir and evacuation channel. Right: Disposition of water level (US) and velocity (UVP) measuring sections

Starting from an initially flat bed, sediment was fed at the upstream end of the flume. The sediment supply was adjusted during the tests in order to maintain both, uniform flow and equilibrium transport conditions in the approach channel upstream of the weir. The water depth was recorded by the use of 15 ultrasonic gauges (US). The 2D velocity field was

measured with an Ultrasonic Doppler Velocity Profiler (UVP). The final bed topography was determined using digital photogrammetry (Rosier et al., 2004).

With respect to geometric and hydraulic conditions, the initial (!) bottom slope (S_0) varied between 0.1 and 0.4 %, the upstream discharge (Q_1) comprised a range of 0.098 to 0.222 m^3/s. The initial (!) crest height (w_D) was fixed to 0.10 m. Regarding the crest length (L_D), values of 3.00 m (test series B), 6.00 m (test series C) and two times 2.50 m (= 5.00 m) (test series D) were tested.

MEASURED OUTFLOW ANGLES

Lateral outflow angles, defined as $\tan \phi_D = v_y / v_x$ with v_x flow velocity in longitudinal direction (channel axis) and v_y flow velocity in transverse direction (see Fig. 1d and insert in Figs 3 and 4 for definition), have been determined using the flow velocities (v_x, v_y) for the entire overflow water depth. In general this has been the part between z / y = 0.75 and 1.00 or approximately the upper 1/4 of the total flow depth (y). In Fig. 3 typical velocity profiles close to the side overflow are presented. The UVP-probes used for the determination of $\tan \phi_D$ are located at y_B = 1.20 m, thus not on the crest of the side weir but 0.30 m towards the channel centre line (Fig. 2, right). In Tab. 1 measured outflow angles for the three test series are presented.

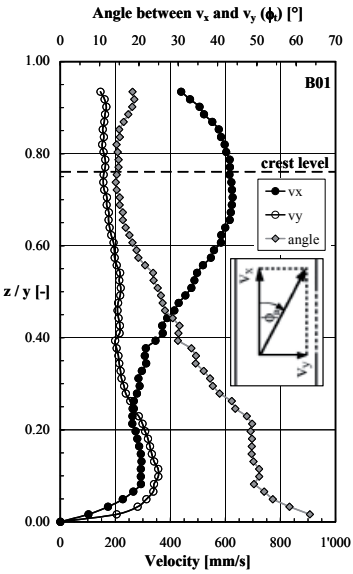

A typical streamwise evolution of the outflow angle is depicted in Fig. 4. It can be seen that up- and downstream of the weir the angle is close to zero. In the weir alignment the outflow angel increases towards its maximum located at $x_{\phi D,max}$ = 7.00 m or 2/3 L_D (L_D weir crest length) before decreasing towards the downstream weir corner. With respect to the entire data set (test series B, C and D), the location of the maximum outflow angle is represented by the ratios $x_{\phi D,max}/L_D$ = 0.72 (test series B), 0.80 (test series C) and 0.78 (test series D). This means that the location of the maximum outflow angle is shifted towards the downstream weir corner with increasing weir length.

Fig. 3: 2D-velocity distribution and torsion angle ϕ_t between v_x and v_y close to the side overflow for experiment B01. The torsion angle in the overflow region above the crest level corresponds to the lateral overflow angle ϕ_D. The streamwise location of the profiles is at x = 8.00 m (downstream weir corner, see Fig. 1, right), the lateralwise position at y_B = 1.20 m. The flow depth at y_B = 1.20 m has been y = 12.5 cm, the mean flow depth for the entire cross section y = 14.8 cm

The average location of the maximum outflow angle starting from the beginning of the weir might be expressed by the relation:

$$\frac{x_{\phi D,\max}}{L_D} = 0.76 \approx 3/4 \quad \text{or} \quad x_{\phi D,\max} \approx 3/4\, L_D \tag{10}$$

The location of the maximum outflow angle is close to the location of the maximum elevation of the local sedimentary deposit forming in the weir reach.

Tab. 1: Measured lateral outflow angles ϕ_D along the weir crest

Test series	**Minimum ϕ_D** [°]	**Maximum ϕ_D** [°]	**Mean ϕ_D** [°]
B	-4	24	7
C	-1	4	2
D	-5	17	4
average	-3	15	4

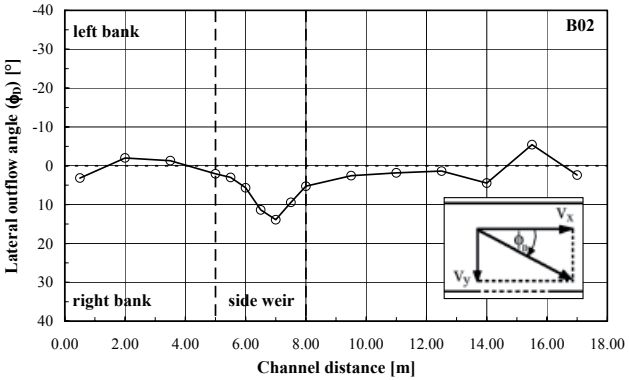

Fig. 4: Example of the streamwise evolution of the lateral outflow angle ϕ_D (plan view). The location of the side weir is on the right bank

MEASURED VERSUS PREDICTED OUTFLOW ANGLES FROM LITERATURE

To compare measured outflow angles from the present investigation with relations from literature the approaches by Subramanya & Awasthy (1972) and Hager (1987) are considered.

Using the approach Froude number at the upstream weir corner (Fr_1), Subramanya & Awasthy (1972) propose the following expression for the deflection angle (ϕ_D) (see also Eq. 7, repeated here):

$$\sin\phi_D = \sqrt{1 - \frac{3Fr_1^2}{2 + Fr_1^2}} \tag{11}$$

Introducing the following dimensionless variables:

$$N = \frac{y_1}{E_1} \quad \text{and} \quad M = \frac{w_D}{E_1} \tag{12}$$

with N relative flow depth, M relative weir height, y_1 flow depth at the upstream weir corner, E_1 specific energy at the upstream weir corner and w_D weir height, the lateral outflow angle for a prismatic, nearly horizontal side weir is given by Hager (1987):

$$\sin \phi_D = \sqrt{\frac{N - M}{3 - 2N - M}} \tag{13}$$

In Tab. 2 mean outflow angles resulting from the two approaches described above are summarized and compared with measured outflow angles from the present study.

Tab. 2: Comparison of measured lateral outflow angles ϕ_D with two approaches from literature

Author	**Minimum ϕ_D** [°]	**Maximum ϕ_D** [°]	**Mean ϕ_D** [°]
Subramanya & Awasthy (1972)	10	48	33
Hager (1987)	17	30	25
present study	-3	15	4

Tab. 2 indicates that measured deflection angles from the present study are significantly smaller than those computed by approaches from literature. Regarding the approach of Subramanya & Awasthy (1972) measured angles only amount to 4/33 = 12 % of computed values. For Hager (1987) this ratio is 4/25 = 16 %. Moreover, Hager (1987) stated measured values in the range of $\phi_D = 26° \div 50°$.

The difference between computed and measured angles is mainly due to different geometric and hydraulic boundary conditions, e. g. different L_D/B- and y_1/L_D-ratios, horizontal bottom slope, non-movable bed and restricted outflow conditions, weirs of zero height ($w_D = 0.00$ m), weirs with dead end ($Q_D = Q_1$, downstream main-channel discharge $Q_2 = 0.00$ m^3/s) and different Froude numbers (Fr_1). With respect to measured Froude numbers comparatively high values are observed ($0.50 \leq Fr_1 \leq 1.00$, mean Froude number $Fr_1 = 0.79$). This means the longitudinal velocity component is much greater than the lateral one ($v_x >> v_y$), resulting in small lateral outflow angles.

For $Q_D/Q_1 < 0.50$, being the case for the present study, El-Khashab & Smith (1976) reported that a considerable part of the approach flow remains in the main channel and that there is a strong forward velocity which has a dominant effect on flow conditions. Moreover, as stated above, the UVP-probes used for the determination of ϕ_D are located at $y_B = 1.20$ m, thus not on the crest of the side weir but 0.30 m towards the channel centre line.

DEVELOPMENT OF A NEW APPROACH FOR LATERAL OUTFLOW ANGLES

Since the two approaches from literature do not properly reflect the results of the present study, a new and more appropriate relation for mean outflow angles at high discharges and (implicitly!) mobile bed conditions is developed.

Within this context the outflow angle is supposed to be a function of channel and side weir geometry as well as flow conditions. To account for flow conditions the Froude number (Fr_1)

is expected to represent an adequate parameter. Finally, the outflow angle is assumed to depend on a product of power relationships of the type:

$$\sin\phi_D = f(x_i) = f\left(x_1^{\alpha}\ x_2^{\beta}\ x_3^{\gamma}\ x_4^{\delta}\ x_5^{\varepsilon}\right) \tag{14}$$

Using dimensional analysis, the coefficients x_1 through x_5 were found to be $x_1 = Q_1$, $x_2 = g$, $x_3 = B$, $x_4 = L_D$ and $x_5 = Fr_1$. The exponents α to ε were determined to be $\alpha = 1$, $\beta = -1/2$, $\gamma = -1/2$, $\delta = -2$ and $\varepsilon = -1$. Hence, Eq. 14 reads:

$$\sin\phi_D = f(x) = f\left(Q_1\ \frac{1}{\sqrt{g}}\ \frac{1}{\sqrt{B}}\ \frac{1}{L_D^2}\ \frac{1}{Fr_1}\right) \tag{15}$$

Finally, by curve fitting, a linear relationship has been identified:

$$\sin\phi_D = f(x) = 16.91\,x + 0.02 \tag{16}$$

Resuming, the following expression for the determination of lateral outflow angles at high discharges and (implicitly) mobile bed conditions is proposed:

$$\sin\phi_D = f(x) = 16.91\left(\frac{Q_1}{\sqrt{g\,B}\,L_D^2}\ \frac{1}{Fr_1}\right) + 0.02 \tag{17}$$

Note that the term $Q_1/((g\,B)^{1/2}L_D^2)$ is defined like a Froude number. The R^2-value of Eq. 17 is 0.75.

With $Q_1 = v_1\,B\,y_1$ and $Fr_1 = v_1/(g\ y_1)^{1/2}$ Eq. 17 might be expressed as:

$$\sin\phi_D = f(x) = 16.91\left[\left(\frac{B}{L_D}\right)^{1/2}\left(\frac{y_1}{L_D}\right)^{3/2}\right] + 0.02 \tag{18}$$

Since the ratio y_1/L_D in Eq. 18 is raised to the power of 3/2, the influence of flow conditions (y_1) is of greater importance than the channel geometry (B), raised to the power of 1/2.

With respect to extreme values for $x = 0.00$, e. g. a long weir crest (L_D) and B and y_1 = constant, Eq. 18 yields $\sin\phi_D = 0.02$ representing a rather negligible outflow angle of $\phi_D = 1.15°$. For great x-values the maximum of $\sin\phi_D$ is given by 1.00 ($\phi_D = 90°$). This condition is achieved for $x = 0.06$. Consequently, the (theoretical) application range of Eq. 18 is $0.00 \le x \le 0.06$ and $0.02 \le f(x) \le 1.00$ (valid for $0.25 \le B/L_D \le 0.50$ and $0.014 \le y_1/L_D \le 0.049$).

Eq. 17 (or Eq. 18) has been developed on the basis of measured outflow angles at $y_B = 1.20$ m, thus not immediately at the weir but 0.30 m towards the channel center line (Fig. 2, right). To estimate the outflow angle near the weir a logarithmic or linear extrapolation procedure is suggested. The choice of a logarithmic or linear extrapolation depends on the shape of the spanwise velocity distribution in the x-y-plane (plan view). Hence, computed angles according to Eq. 17 (or Eq. 18) might be increased by a factor of 1.33 (logarithmic) or 1.52 (linear) to obtain the outflow angle near the weir ($y_B \approx 1.50$ m):

logarithmic extrapolation: 1.33 (19)

linear extrapolation: 1.52

In contrast to the approaches of Subramanya & Awasthy (1972) and Hager (1987) an advantage of Eq. 17 (or Eq. 18) is the explicit appearance of the channel geometry (B), the side weir geometry (L_D) and flow conditions (Q_1, Fr_1, y_1). In Eq. 11 only flow variables (Fr_1) occur, whereas in Eqs 12 and 13 only flow conditions (y_1, E_1) and weir geometry (w_D) interfere.

DISCUSSION OF RESULTS AND APPLICATION RANGE

As it has been mentioned before rather elevated discharges as encountered in high flood seasons have been studied. Therefore, comparatively high Froude numbers have been observed ($0.50 \leq Fr_1 \leq 1.00$, mean Froude number $Fr_1 = 0.79$). This means the longitudinal velocity component is much greater than the lateral one, resulting in small lateral outflow angles. For Q_D/Q_1 - ratios < 0.50 (Q_D spill discharge), a considerable part of the approach flow remains in the main channel and there is a strong forward velocity which has a dominant effect on flow conditions. In the present study the ratio of Q_D/Q_1 varied between 0.06 and 0.37 with a mean value of 0.21.

The effects of sediment aggradation, local sediment deposition in the weir reach and the formation of bed forms are implicitly included in the new expression, since it is based upon final values at the end of the experiments when dynamic equilibrium conditions were achieved.

As being usual for experimental investigations the application range of the proposed relation is given by the experimental boundary conditions under which the approach has been developed. Regarding the main-channel and weir geometry, the application limits can be derived from the bottom slope varying between $0.1\ \% \leq S0 \leq 0.4\ \%$ and the ratio of side weir crest length to main-channel width being $2.00 \leq L_D/B \leq 4.00$. As far as the properties of the mobile bed material are concerned the relative roughness y_1/d_{90} ranged from 40 to 70 (y_1 flow depth, d_{90} grain size for which 90 % of the sediment is finer by weight). The flow regime has always been subcritical with Froude numbers $0.50 \leq Fr_1 \leq 1.00$. The ratio of overflow to approach discharge was in the range of $0.06 \leq Q_D/Q_1 \leq 0.37$.

CONCLUSIONS

The interaction of a side weir overflow with bed-load transport and bed morphology in a channel has been studied experimentally. Due to the lateral loss of water in the main-channel the sediment transport capacity decreases and aggradation and local sediment deposition occurs in the downstream weir alignment. As a consequence, the flow depth in the main-channel as well as on the weir increases and the side overflow discharge as well. Since side overflow devices such as side weirs or overflow dams on rivers usually enter into operation in flood situations, the approach discharges studied have been rather high and elevated subcritical Froude numbers have been observed.

The morphological phenomena taking place have a considerable impact on the overflow conditions. In this context the lateral outflow angle plays an important role, since the overflow angle might be incorporated in the determination of the side weir discharge coefficient, thus influencing the intensity of the side overflow.

The experiments revealed that existing approaches from literature for the determination of the lateral outflow angle do not seem to be appropriate for the boundary conditions of the present

study. The substantial difference of the present investigation is the presence of mobile bed conditions and rather high discharges. Therefore, a new approach based on a systematic flume study has been developed. The main input variables are referring to parameters from main-channel and side weir geometry as well as flow conditions. The input variables and the application range are given by dimensionless ratios, thus facilitating the transfer from the experimental boundary conditions to prototype conditions and the use in engineering practice.

REFERENCES

El-Khashab, A., Smith, K. V. H. (1976): „Experimental investigation of flow over side weirs". Journal of the Hydraulics Division, 102 (9): 1255-1268.

Favre, H. (1933): „Contribution à l'étude des courants liquides". Rascher et Cie, Zurich.

Hager, W. H. (1987): „Lateral outflow over side weirs". Journal of Hydraulic Engineering, 133 (4): 491-504.

Rosier, B., Boillat, J.-L., Schleiss, A. J. (2004): „Mapping of bed morphology for lateral overflow using digital photogrammetry". 2nd International Conference on Scour and Erosion – ICSE 2, Singapore, Singapore.

Sinniger, R. O., Hager, W. H. (1989): „Constructions hydrauliques". Traité de Génie Civil, Vol. 15, Presses polytechniques et universitaires romandes, Lausanne, Switzerland.

Subramanya, K., Awasthy, S. C. (1972): „Spatially varied flow over side weirs". Journal of the Hydraulics Division, 98 (1): 1-10.